Construction of m6A-related ceRNA networks via epitranscriptomic profiling and their association with immune infiltration in lung adenocarcinoma

Zhuohui Tan¹, Chunhong Fan¹, Limei Zhu¹, Tingting Liu^{2*}

¹Department of Respiratory and Critical Care Medicine, The Affiliated Shunde Hospital of Jinan University, Foshan, Guangdong Province, China

²Department of Respiratory and Critical Care Medicine, The First Affiliated Hospital of Xi'an Jiaotong University, Xi'an, China

Submitted: 14 July 2025; Accepted: 8 September 2025

Online publication: 7 November 2025

Arch Med Sci DOI: https://doi.org/ 10.5114/aoms/210481 Copyright © 2025 Termedia & Banach

Abstract

Introduction: The N6-methyladenosine (m6A)-related competing endogenous RNA (ceRNA) network plays a critical role in the occurrence and progression of lung adenocarcinoma (LUAD). This study aimed to investigate the characteristics of m6A-related ceRNAs.

Material and methods: Gene expression matrices and clinical data were obtained from The Cancer Genome Atlas (TCGA) database, along with the GSE176348 dataset sourced from the Gene Expression Omnibus (GEO) database. Differential expression analysis was performed using the "GEO2R" tool and the "limma" R package to identify differentially expressed genes (DEGs). By integrating results from CIBERSORTx and m6A-related databases, we further identified m6A-associated and immune-related genes. The tumor immune microenvironment (TIME) was characterized utilizing the TIMER and TISIDB databases. Finally, differential expression of key molecules between LUAD and normal lung tissues was validated through polymerase chain reaction (PCR).

Results: We found 220 DEGs related to multiple classical tumor pathways using the DAVID and Metascape databases, such as regulation of ERK1, ERK2 cascade, PI3K-AKT signaling pathway and regulation of cell adhesion. By combining the m6A and CIBERSORTx databases, we selected ANGPT1, which was involved in the PI3K-AKT pathways. ANGPT1 expression was lower in LUAD cells than in normal lung cells and associated with patients' prognosis (p < 0.01). ANGPT1 expression was correlated with PD-L1 (p < 0.01) and multiple immune cells. The PCR results showed that ANGPT1 was expressed at significantly lower levels in A549 cells than in BEAS-2B cell lines.

Conclusions: A validated signature of the m6A-related ceRNA network demonstrated prognostic utility for predicting survival and provides new insights into potential novel therapeutic targets.

Key words: N6-methyladenosine, competing endogenous RNA, tumor immune microenvironment, polymerase chain reaction.

Introduction

Lung cancer is the leading cause of cancer-related deaths world-wide [1–3]. Non-small cell lung cancer (NSCLC) accounts for 80% of all lung cancer patients, more than half of whom are elderly patients [4]. Although comprehensive treatment strategies, including surgery, ra-

*Corresponding author:

Tingting Liu
Department of Respiratory
and Critical
Care Medicine
The First Affiliated
Hospital of Xi'an
Jiaotong University
277 Yanta West Road
Xi'an, 710061, China
E-mail: liuting6883@163.com

diotherapy, chemotherapy, targeted therapy, and checkpoint inhibitors, have significantly advanced the management of lung cancer, the 5-year survival rate among patients remains unsatisfactory [5–7]. Therefore, this study was designed to identify novel prognostic molecular biomarkers and therapeutic targets for patients with lung adenocarcinoma (LUAD).

m6A is the most common internal modification of mRNAs and plays an important role in regulating mRNA splicing, localization, translation, stability [8] and biological processes [9]. However, their roles in tumorigenesis remains unclear [10]. Multiple m6A-related studies have been conducted on different cancers, such as ovarian cancer [11], bladder cancer [12], pancreatic cancer [13] and gastric cancer [14]. The ceRNA network links the functions of protein-coding RNAs and non-coding RNAs [15]. Long non-coding RNAs (IncRNAs) are associated with the occurrence of cancers, including DNA methylation, histone modification, cell proliferation, and apoptosis [16].

The tumor immune environment (TME) is important for patients receiving immunotherapy. The T cell-mediated antitumor immune response is the basis of tumor immunotherapy and is associated with a favorable prognosis [17]. In recent years, immune checkpoint inhibitors have been used to treat a variety of cancers and have shown achieved good curative effects [18]. The growing field of immune metabolism has revealed promising indications of metabolic targets to modulate anticancer immunity [19]. However, the TME-related mechanisms in NSCLC remain unclear.

Material and methods

Data collection

The TCGA database (https://portal.gdc.cancer.gov/) includes gene transcriptome data and basic clinical data of patients with LUAD. The GSE176348 was downloaded from the GEO database (https://www.ncbi.nlm.nih.gov/). CIBERSORTX [20] (https://cibersortx.stanford.edu/index.php) is an analytical tool that imputes gene expression profiles and provides an estimation of the abundances of member cell types in a mixed cell population, using gene expression data. The m6A related gene matrix data were downloaded from the m6A2 target database (http://m6a2target.canceromics.org).

Differential expression analysis of mRNAs and lncRNAs

The Arraystar Human m6A-mRNA and m6A-lncRNA epitranscriptomic microarray analysis (GSE176348) was performed on six pairs of LUAD tissues and adjacent non-tumor tissues to com-

pare and screen the m6A-regulated genes of LUAD, thus offering a new avenue for targets and strategies for LUAD diagnosis and treatment. "GEO2R" was used to analyze differentially expressed mRNAs (DEmRNAs) and lncRNAs (DElncRNAs). The R package "limma" was used to explore DElncRNAs of the TCGA database.

Functional enrichment analysis of DEmRNAs in GEO database

We screened out 222 m6A-related DEmR-NAs-encoded proteins, and explored their molecular functions (MF), biological processes (BP), cellular components (CC), and Kyoto Encyclopedia of Genes and Genomes (KEGG) pathways using DAVID (https://david.ncifcrf.gov/). Metascape (https://metascape.org/gp/index.html) was used to further validate the functional enrichment of DEmRNAs.

Survival analysis

We screened the DElncRNAs in TCGA database from "limma" R package. The Venn diagram (http://bioinformatics.psb.ugent.be/webtools/Venn/) was used to analyze differentially expressed m6A-related lncRNAs from the GEO database and DElncRNAs from the TCGA database. The Kaplan-Meier Plotter database (https://kmplot.com/analysis/) was used to explore the prognostic-related DEmRNAs and DElncRNAs.

Construction of m6A-related ceRNA network

Based on the above analysis, we selected the functionally enriched prognostic mRNAs. Four databases were used to identify potential miRNAs: starBase (http://starbase.sysu.edu.cn/starbase2/index.php), TargetScan (http://www.targetscan.org/vert_72/), miRWalk (http://mirwalk.umm.uni-heidelberg.de/), and miRDB (http://mirdb.org/).

Further comprehensive verification of angiopoietin-1

Several databases were used to perform the expression, methylation, mutation, and survival analyses. Ualcan [21] (http://ualcan.path.uab.edu) and TNM plot (https://tnmplot.com/analysis/) show the expression of ANGPT1 in LUAD and pan-cancer. We studied the correlation between the ANGPT1 expression and cancer stage, patient race, sex, age, and smoking habits. GEPIA (http://gepia.cancer-pku.cn) showed the chromosome location of ANGPT1 and expression. Prognostic related analyses were performed using the Progno-Scan software. Meta-analysis effectively combines statistical strength from multiple datasets, which

allows for greater precision than using any single study. Forest plots were constructed to summarize the tumor—normal standardized mean difference for tumor vs normal meta-analysis and hazard ratios for survival meta-analysis of lung cancer (https://lce.biohpc.swmed.edu/lungcancer/metagenename.php). We also explored the ANGPT1 methylation levels in LUAD using MEXPRESS (https://mexpress.be/old/mexpress.php) and Fire-Browse (http://firebrowse.org/).

Immune infiltration analysis of ANGPT1 in LUAD

The Tumor Immune Estimation Resource (TIMER) database (https://cistrome.shinyapps.io/ timer/) is a comprehensive resource for systematical analysis of immune infiltrates across diverse cancer types. This version of the webserver provides immune infiltrates' abundances estimated using multiple immune deconvolution methods. We compared ANGPT1 expression levels and immune cell infiltration between normal and LUAD tissues. Correlations between ANGPT1 expression and various immune cells, such as B cells, CD4+ T cells, CD8+ T cells, macrophages, neutrophils, and dendritic cells, were analyzed. TISIDB (http://cis.hku.hk/TISIDB/) is an integrated repository portal for tumor-immune system interactions. TISIDB was used to analyze the association between ANGPT1 expression and abundance of tumor-infiltrating lymphocytes (TILs).

Construction of ANGPT1-related immune co-expression gene network

Using the cBioPortal database (https://www.cbioportal.org/), we explored ANGPT1-related genes. The Coexpedia (https://www.coexpedia.org/search.php) database was used to identify ANGPT1-related co-expression genes. Additionally, we analyzed the correlation of gene expression and immune cell infiltration in the CIBERSORT database.

ANGPT1 expression was verified by polymerase chain reaction (PCR)

We performed PCR verification in normal pulmonary bronchial epithelial cells (BEAS-2B cell line) and the LUAD cell line (A549, H1299). Professional PCR instruments were used to count CT values. GraphPad Prism (https://www.graphpad.com/scientific-software/prism/) was used for analysis of data. The experiments were conducted in triplicate.

Statistical analysis

Differential expression analysis between LUAD and normal tissues was performed using the R package "limma". Genes with an adjusted *p*-value (Ben-

jamini-Hochberg method) < 0.01 and an absolute \log_2 fold change $|\log FC| > 1$ were considered statistically significant and defined as DEGs. For survival analysis, the Kaplan-Meier method and the log-rank test were used to assess significance, with a p-value < 0.05 considered significant. Correlation analyses (e.g., between ANGPT1 expression and immune cell infiltration) were conducted using Spearman's correlation method. Results are presented with correlation coefficients (r) and p-values. A p-value < 0.05 was considered statistically significant for all analyses unless otherwise specified

Results

Identification of DEmRNAs and DElncRNAs in LUAD patients

The overall workflow of the study is shown in Figure 1. "GEO 2R" was used to analyze DEm6A-related genes from the GEO database. A total of 220 DEmRNAs and 23 DElncRNAs were included according to the screening criteria, p < 0.01 in the volcano plot (Figures 2 A, B). The R package "limma" was used to analyze DElncRNAs in TCGA database. Up-regulated and down-regulated genes are shown in a histogram (Figure 2 D). The common lncRNAs were identified in a Venn diagram; 3 IncRNAs (ACO08268.1, AFAP1-AS1, BLACAT1) were considered (Figure 2 C). Through K-M plotter, AFAP1-AS1, and BLACAT1 were significant for the survival of patients with lung adenocarcinoma (p < 0.01) (Figures 2 E, F). Combining the m6A-related database and immune database, we found that DEmRNAs and DElncRNAs were associated with m6A modification and immune response levels.

Function enrichment analyses of DEmRNAs in GEO database

Metascape software was used to analyze the function of 220 DE mRNAs. We found that these DEmRNAs were associated with many cancer-related signaling pathways, e.g. regulation of ERK1, ERK2 cascade; the PI3K-AKT signaling pathway; and regulation of cell adhesion (Table I, Figure 3 A). Numerous genes were interrelated with each other through the network, such as ANGPT1, NCK1, KDR, FGFR4, ERBB2, FGF2, FGF1, and others (Figures 3 B–E). The DAVID database identified the GO, BP, CC, MF, and KEGG of DE mRNAs. We identified participation of the targeted molecule ANGPT1 in the PI3K-AKT signaling pathway.

Construction of ANGPT1-related ceRNA network

K-M plotter revealed that ANGPT1 expression was significant in LUAD tissues and normal tissues (Figure 4 A). StarBase (8 miRNAs), Target-

Scan (533 miRNAs), miRWalk (1945 miRNAs), and mirDB (145 miRNAs) were used to explore ANGPT1-related miRNAs. A Venn diagram [22] was used to identify common miRNAs associated with ANGPT1, and hsa-mir-448 was included in the above 4 databases (Figure 4 B). Mir-448 expression was higher in LUAD tissues than normal lung tissues and it was associated with the prognosis of LUAD patients (Figure 4 C).

Further expression and immune infiltration level of ANGPT1

ANGPT1 expression was lower in multiple cancers than normal tissues, such as BLCA, BRCA, CESC, COAD, KIRC, KIRP, LUAD, LUSC, PAAD, PRAD,

READ, SARC, SKCM, THCA, THYM, STAD, and UCEC (p < 0.01) (Figure 4 D). Next, we explored the correlation between ANGPT1 expression and patients' race, sex, age (higher expression in older people), smoking habits (lower expression in smoker), TP53 mutation status (lower expression in TP53 mutation), individual cancer stages (the later the stage, the lower the ANGPT1 expression) (p < 0.01) (Figures 4 E–J). ANGPT1 is a protein-coding gene, located at 8q23.1 (Figure 5 A). ANGPT1 expression was lower in 483 tumor tissues than 347 normal lung tissues (Figures 5 B, C). The prognostic relevance of ANGPT1 was further verified by PrognoScan (Figure 5 D). A meta-analysis showed that ANGPT1 was significant in dif-

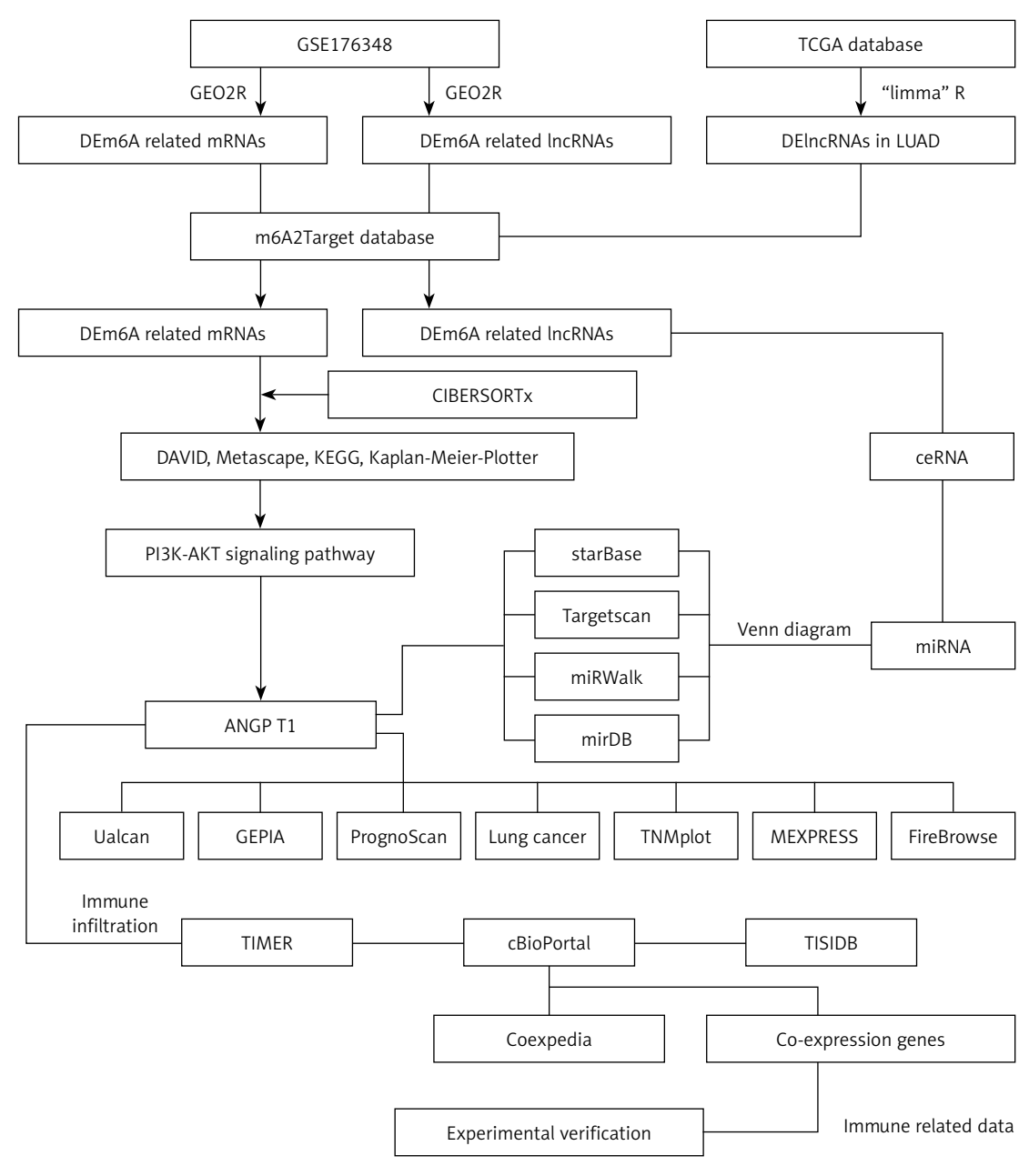


Figure 1. Flow chart of the whole study

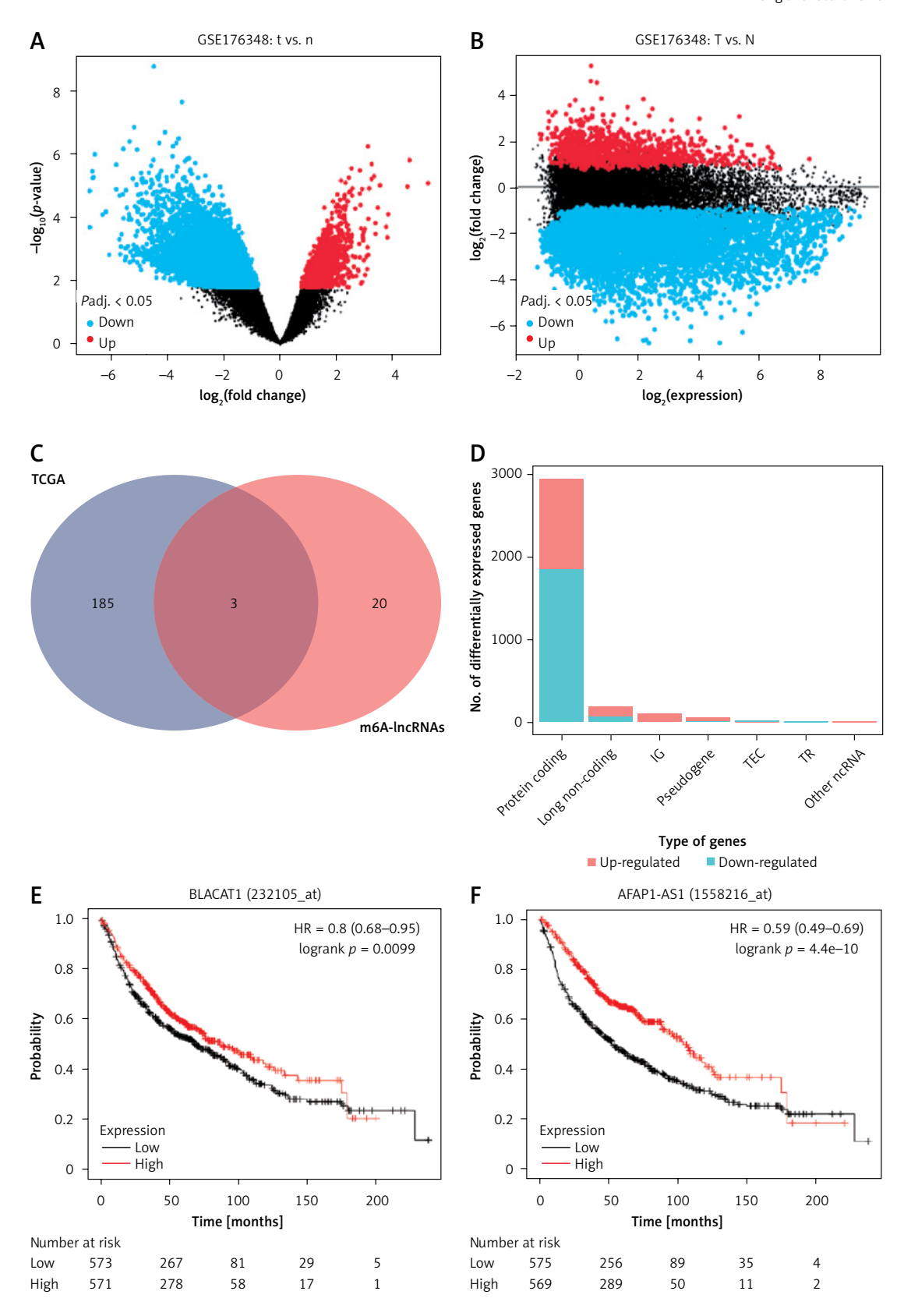


Figure 2. Differentially expressed m6A-related mRNAs and lncRNAs in LUAD. **A**, **B** – DE mRNAs of GEO database are shown in volcano plots. **C** – Three m6A-related lncRNAs were explored in TCGA and GEO databases. **D** – Distribution of differential genes (protein coding RNAs, long non-coding RNAs and other ncRNAs) in TCGA database. **E**, **F** – Survival curves of two long non-coding RNAs (AFAP1-AS1, BLACAT1)

Table I. Function enrichment analyses of DEmRNAs in GSE176348 from GEO database

GO	Category	Description	Count	%	Log ₁₀ (p)	Log ₁₀ (q)
GO,0048017	GO Biological Processes	Inositol lipid-mediated signaling	11	5.76	-7.34	-2.98
GO,0070372	GO Biological Processes	Regulation of ERK1 and ERK2 cascade	13	6.81	-6.57	-2.72
GO,0001659	GO Biological Processes	Temperature homeostasis	10	5.24	-6.47	-2.72
GO,0050801	GO Biological Processes	Ion homeostasis	20	10.47	-6.29	-2.72
GO,0001822	GO Biological Processes	Kidney development	12	6.28	-6.05	-2.6
GO,0007264	GO Biological Processes	Small GTPase mediated signal transduction	15	7.85	-5.71	-2.38
R-HSA-9012999	Reactome Gene Sets	RHO GTPase cycle	14	7.33	-5.58	-2.3
GO,0003013	GO Biological Processes	Circulatory system process	16	8.38	-5.45	-2.23
GO,0050918	GO Biological Processes	Positive chemotaxis	6	3.14	-5.23	-2.13
R-HSA-5654720	Reactome Gene Sets	PI-3K cascade, FGFR4	4	2.09	-5.04	-2.02
GO,0009617	GO Biological Processes	Response to bacterium	17	8.9	-4.82	-1.97
GO,0030155	GO Biological Processes	Regulation of cell adhesion	17	8.9	-4.8	-1.96
GO,0032970	GO Biological Processes	Regulation of actin filament- based process	12	6.28	-4.74	-1.94
M92	Canonical Pathways	PID angiopoietin receptor pathway	5	2.62	-4.69	-1.93
R-HSA-372790	Reactome Gene Sets	Signaling by GPCR	16	8.38	-4.57	-1.84
ko05418	KEGG Pathway	Fluid shear stress and atherosclerosis	7	3.66	-4.26	-1.64
GO,0048661	GO Biological Processes	Positive regulation of smooth muscle cell proliferation	6	3.14	-4.1	-1.54
hsa00982	KEGG Pathway	Drug metabolism - cytochrome P450	5	2.62	-3.94	-1.45
GO,0006936	GO Biological Processes	Muscle contraction	10	5.24	-3.86	-1.41
GO,0042391	GO Biological Processes	Regulation of membrane potential	11	5.76	-3.7	-1.32

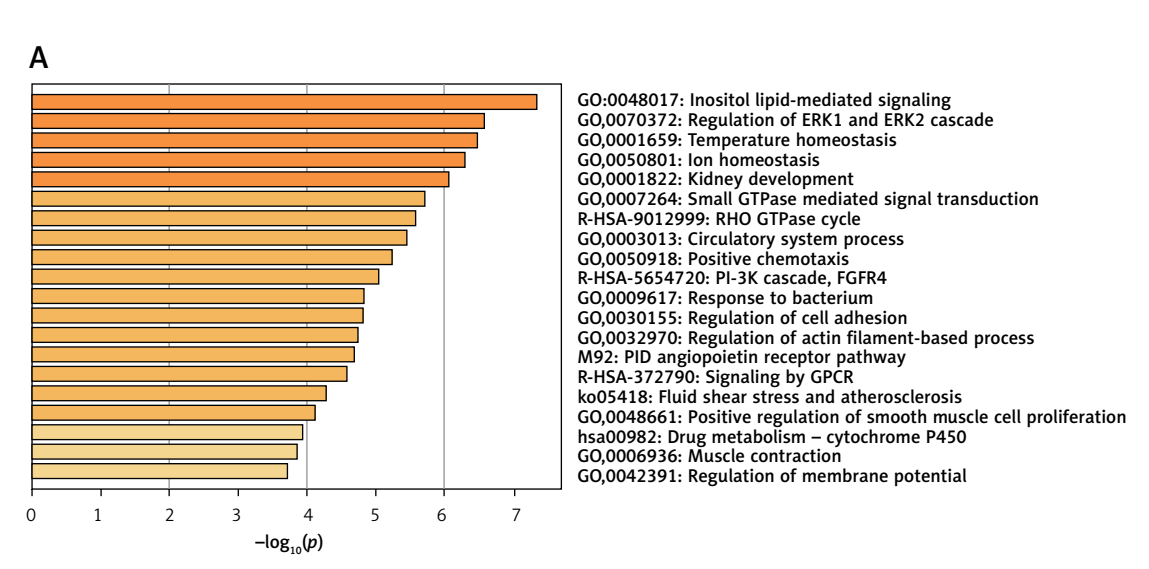


Figure 3. Metascape software was used to analyze functional enrichment of 220 DE mRNAs in the GEO database. A – DEmRNAs were associated with many cancer-related signaling pathways

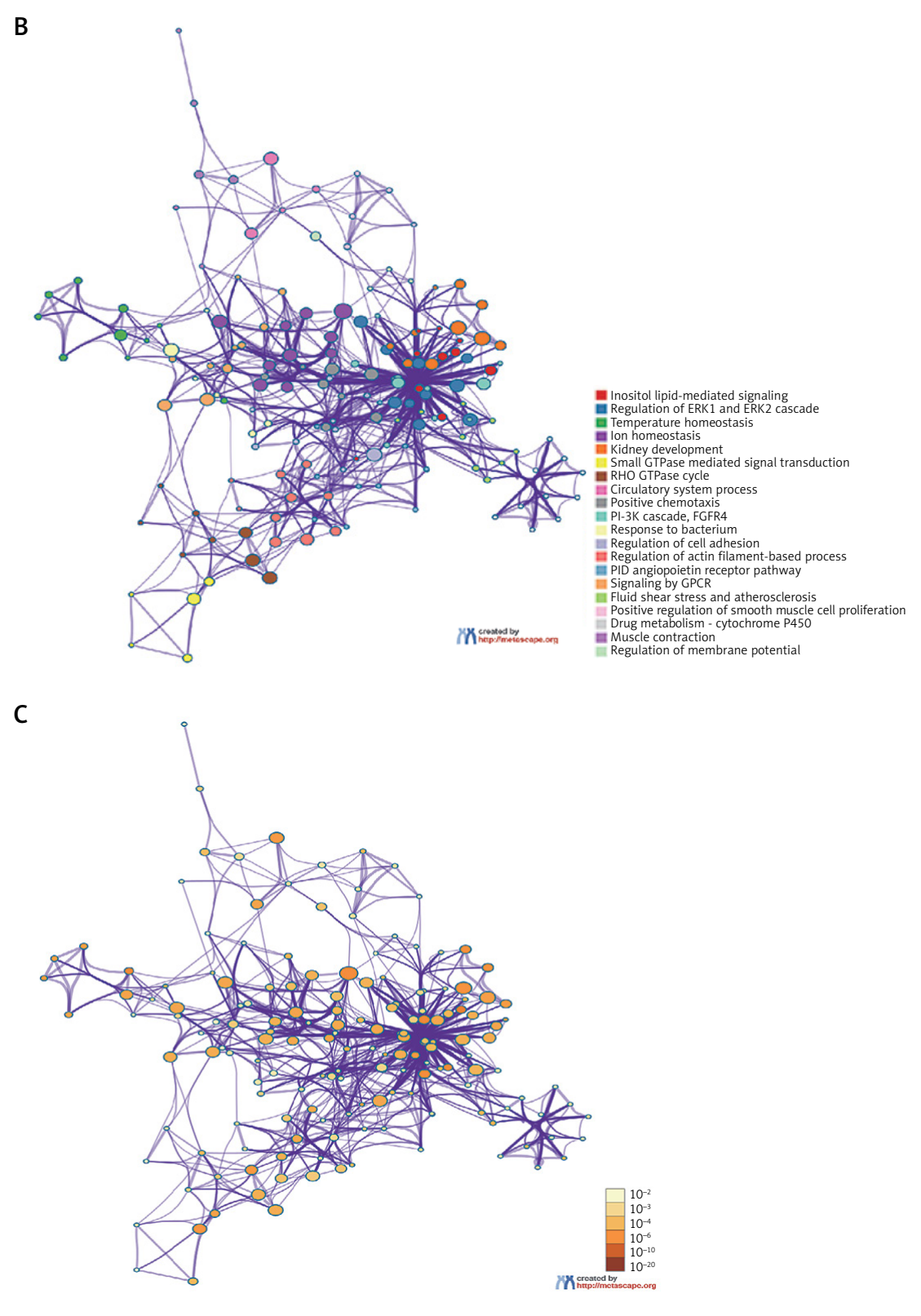
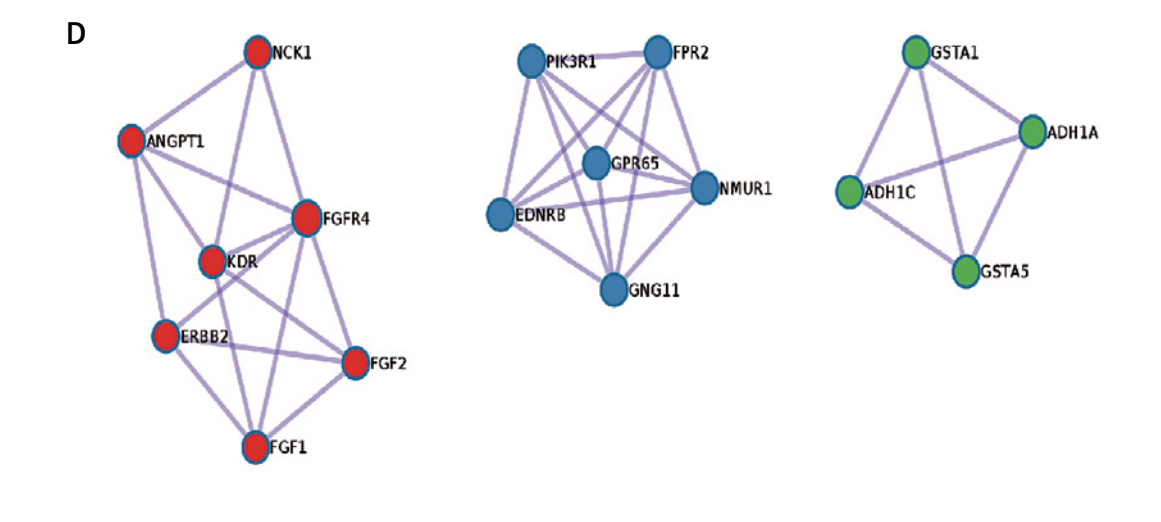
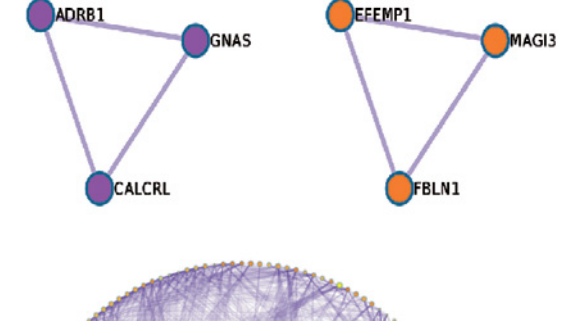


Figure 3. Cont. B – Networks were constructed based on pathways involving differential genes. C – The network was constructed according to the p-values of functional enrichment







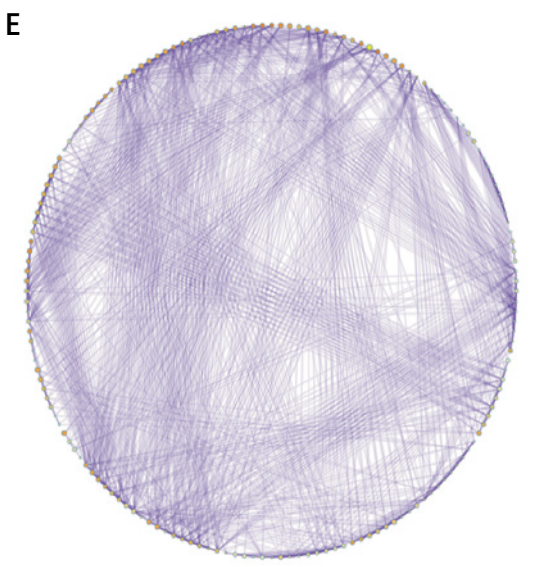


Figure 3. Cont. D – Hub genes were selected using Cytoscape software. E – Functional enrichment results are presented in a circular diagram

ferent LUAD data sets (heterogeneity, $I^2 = 80\%$, p = 0.001; test for overall effect, z = -9.96, p = 2.2e-23) (Figure 5 E). ANGPT1 expression was analyzed in pan-cancer and LUAD (p = 1.59e-118) (Figures 5 F, G). ANGPT1 had different methylation and mutation levels in LUAD (Figures 5 H, I).

Correlation of ANGPT1 expression and immune cell infiltration

The TIMER [23] database was used to analyze ANGPT1 expression in different cancers, and it was

lower in tumor tissues than normal tissues, such as BLCA, BACA, KIAC, KIRP, LUAD, LUSC, and AEAD (Figure 6 A). There was an association between ANGPT1 expression and immune cells, including B cells (p=4.06e-04, CD8+T cells (p=1.35e-12, CD4+T cells (p=6.93e-03), macrophages (p=7.15e-16), neutrophils (p=2.72e-3), and dendritic cells (p=1.16e-07) (Figures 6 B–D) (Table II). We explored whether ANGPT1 expression was associated with PD-L1 reaction. Figures 6 E, F shows the difference in expression between responders and non-responders. Relations between abundance of

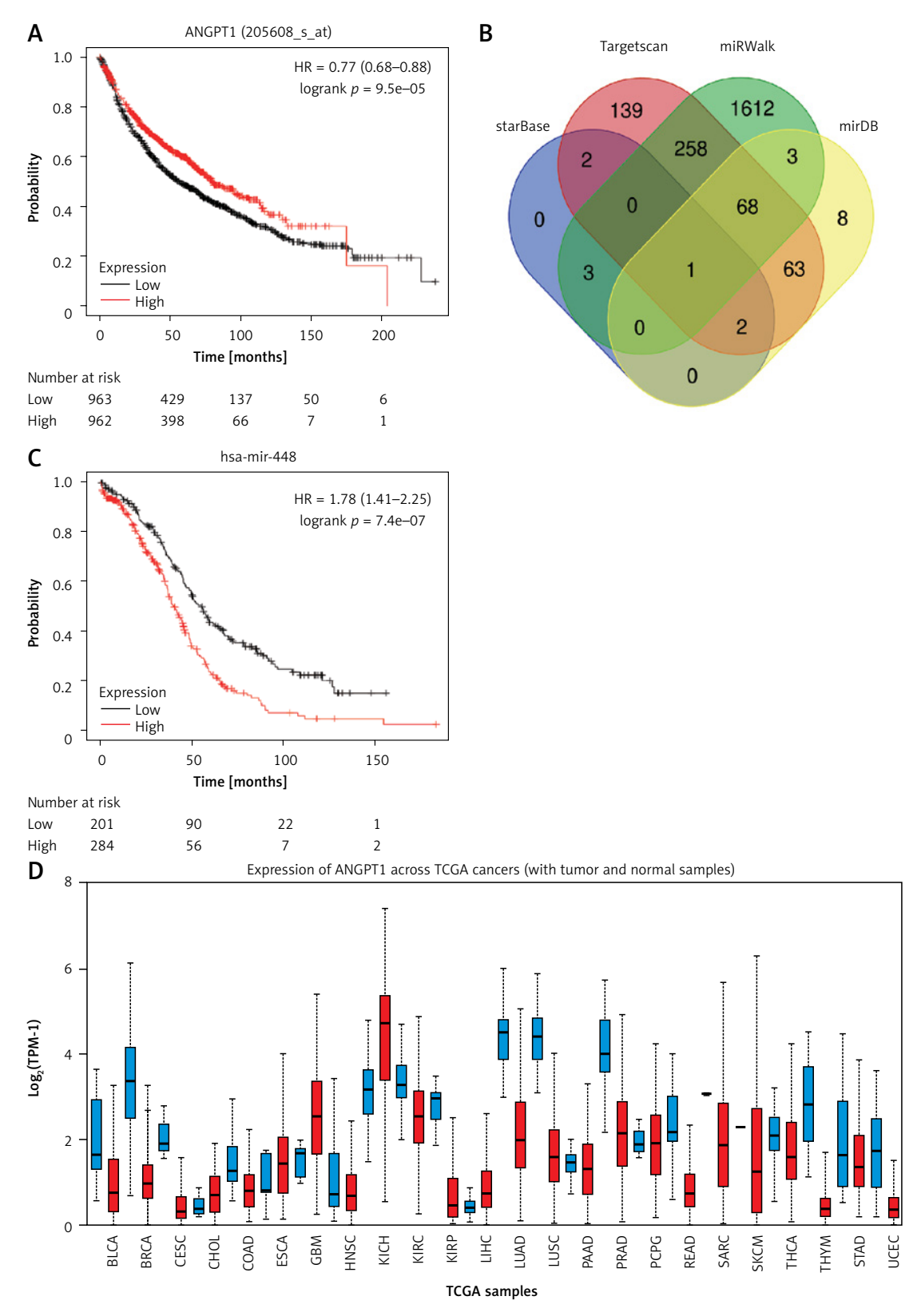


Figure 4. Further analyses of ANGPT1 and construction of ceRNA network in LUAD. A – ANGPT1 expression was lower in LUAD tissues than normal lung tissues (p < 0.01). B – Identification of ANGPT1-related ceRNA network through different databases, such as starBase, TargetScan, miRWalk, mirDB. C – Effect of miRNA448 on survival of patients with LUAD. D – ANGPT1 expression in multiple cancers

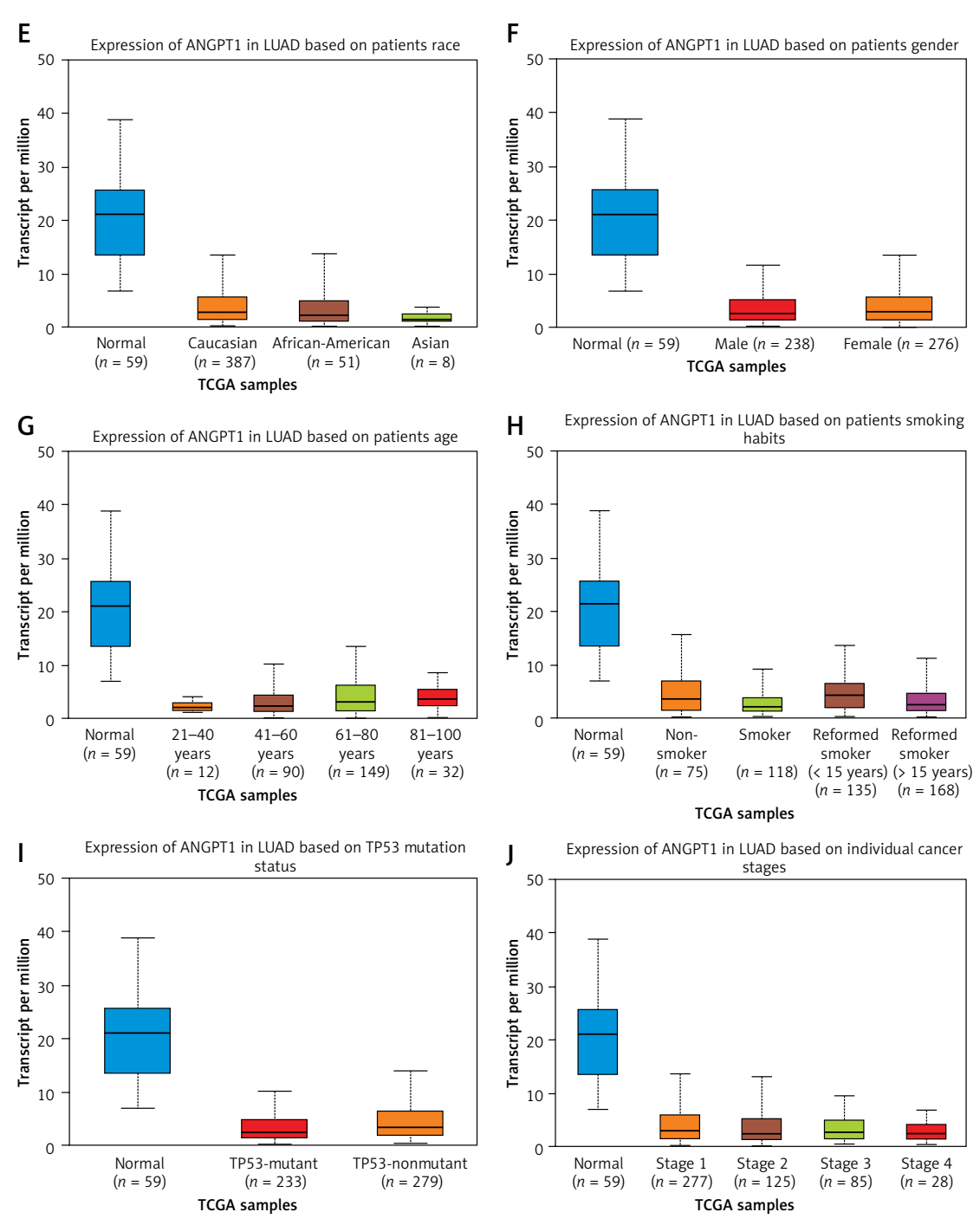


Figure 4. Cont. E–J – Correlation between ANGPT1 expression and LUAD patients' race, sex, age (higher expression in older people), smoking habits (lower expression in smokers), TP53 mutation status (lower expression in TP53 mutation), and individual cancer stages (the later the stage, the lower expression of ANGPT1) (p < 0.01)

tumor-infiltrating lymphocytes (TILs) and expression, copy number, and methylation of ANGPT1 are shown in Figures 6 G–I. There were certain correlations between the expression of ANGPT1 and immune inhibitors and immune stimulators (Figures 6 J, K). Co-expression genes of ANGPT1 were screened using cBioPortal and Coexpedia; combining these with CIBERSORTx, co-expression and immune related genes are shown in Figure 6 L. qRT-PCR verification demonstrated that ANGPT1

expression was lower in tumor tissues (A549 and H1299 cell lines) than normal lung tissues (BEAS-2B cell line) (p < 0.01) (Figure 6 M).

Discussion

In the present study, we identified prognostic m6A-related mRNAs and lncRNAs. GO and KEGG function enrichment revealed classic tumor pathways of these DE genes, such as the PI3K-AKT

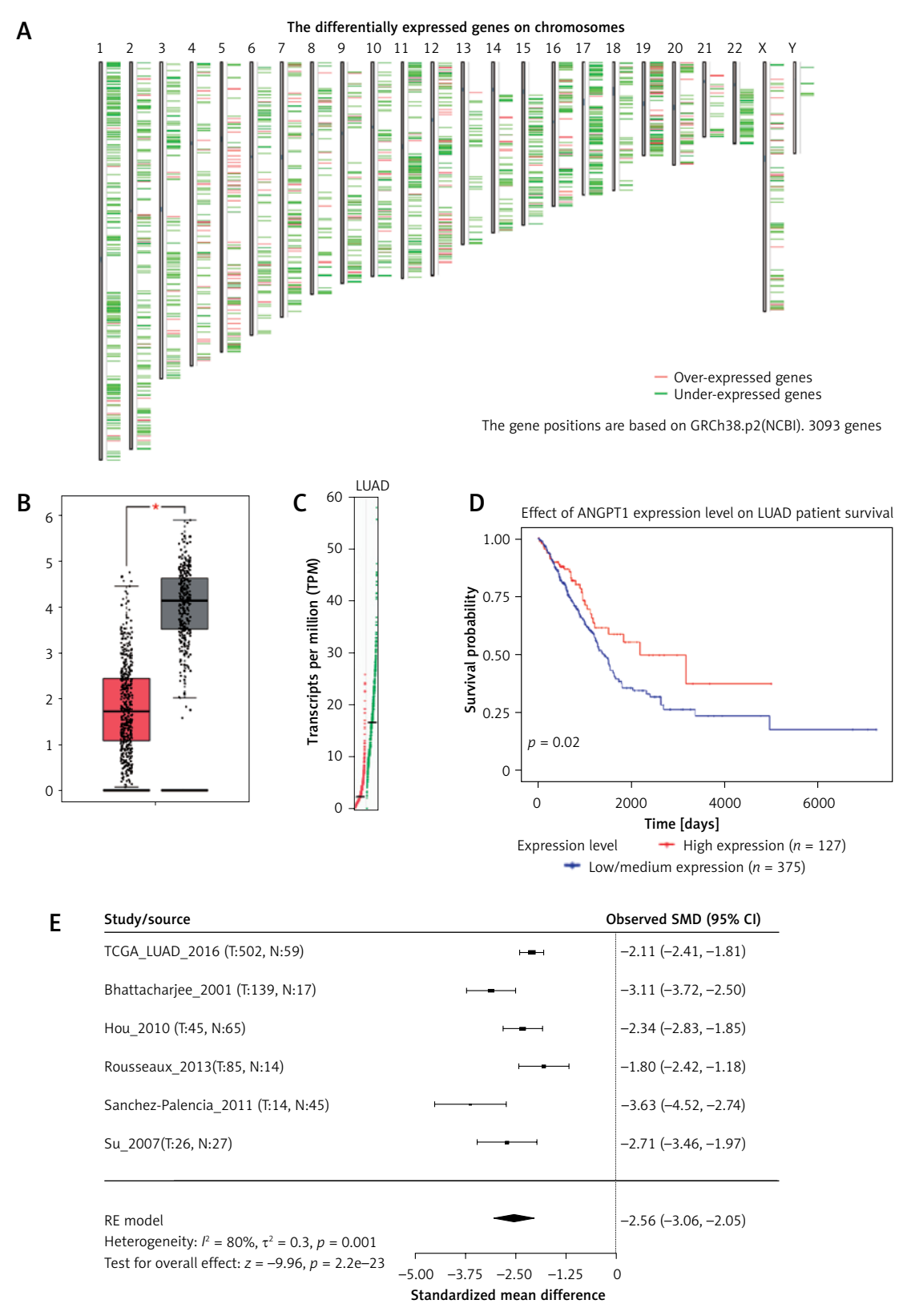


Figure 5. ANGPT1 methylation and mutation analyses in LUAD. A – ANGPT1 is a protein-coding gene, located at 8q23.1. B, C – ANGPT1 expression was lower in LUAD tissues than normal tissues. D – Prognostic relevance of ANGPT1 was further verified using PrognoScan

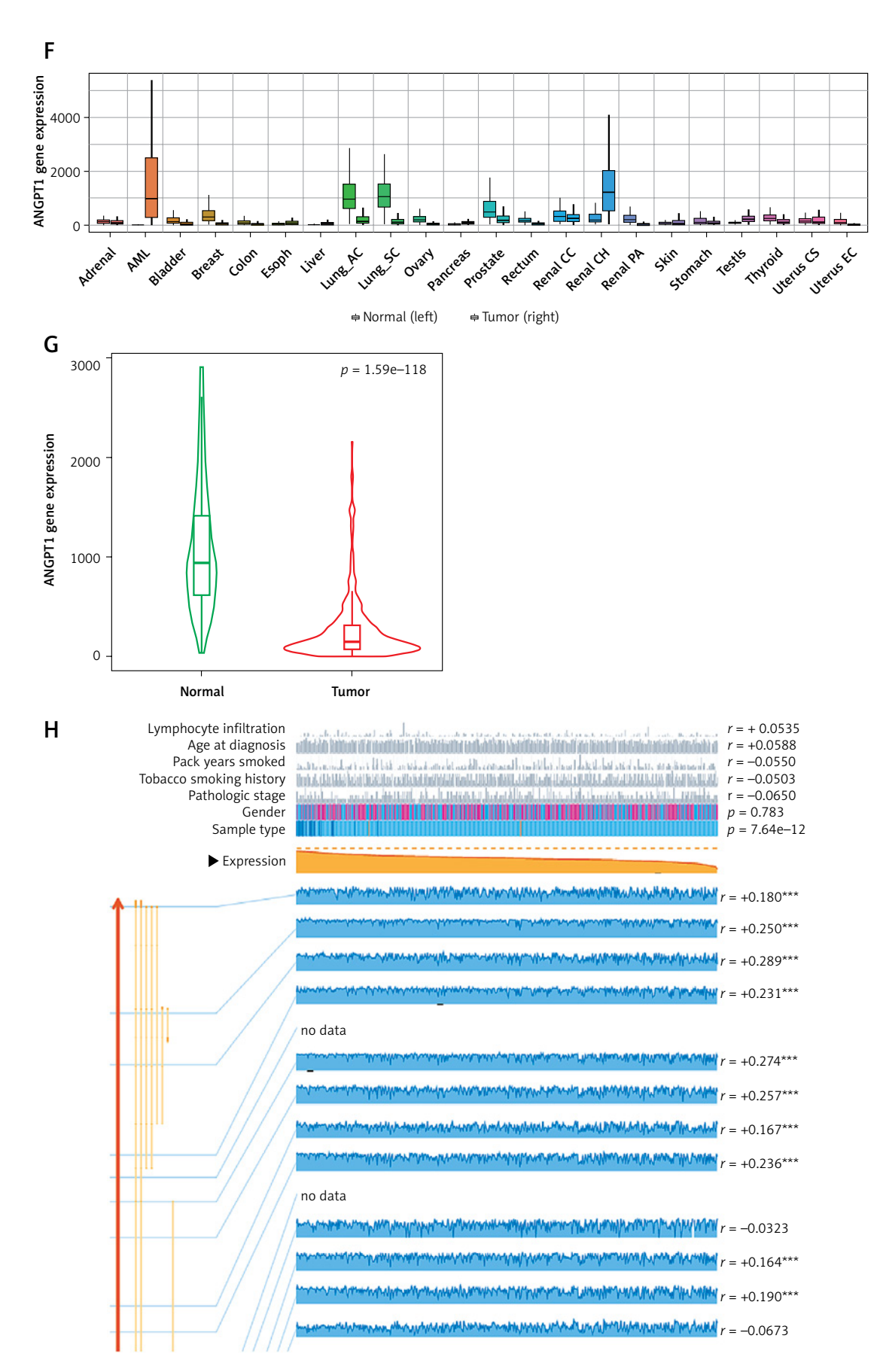


Figure 5. Cont. **F**, **G** – ANGPT1 expression was analyzed in pan-cancer and LUAD, with lung cancer showing p = 1.59e-118. **H** – Associations between ANGPT1 expression and methylation and mutation levels in LUAD

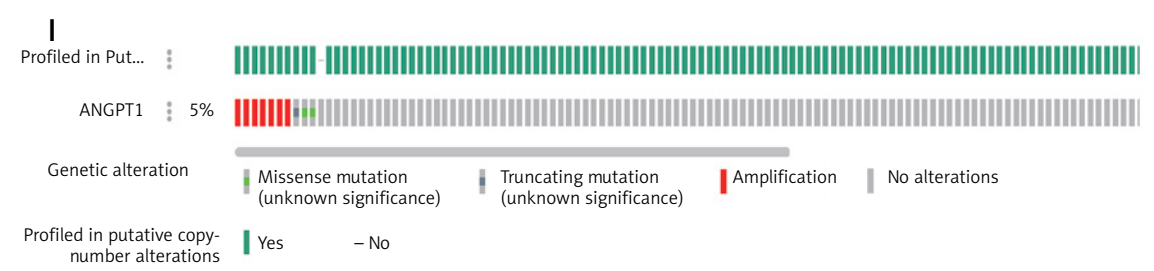
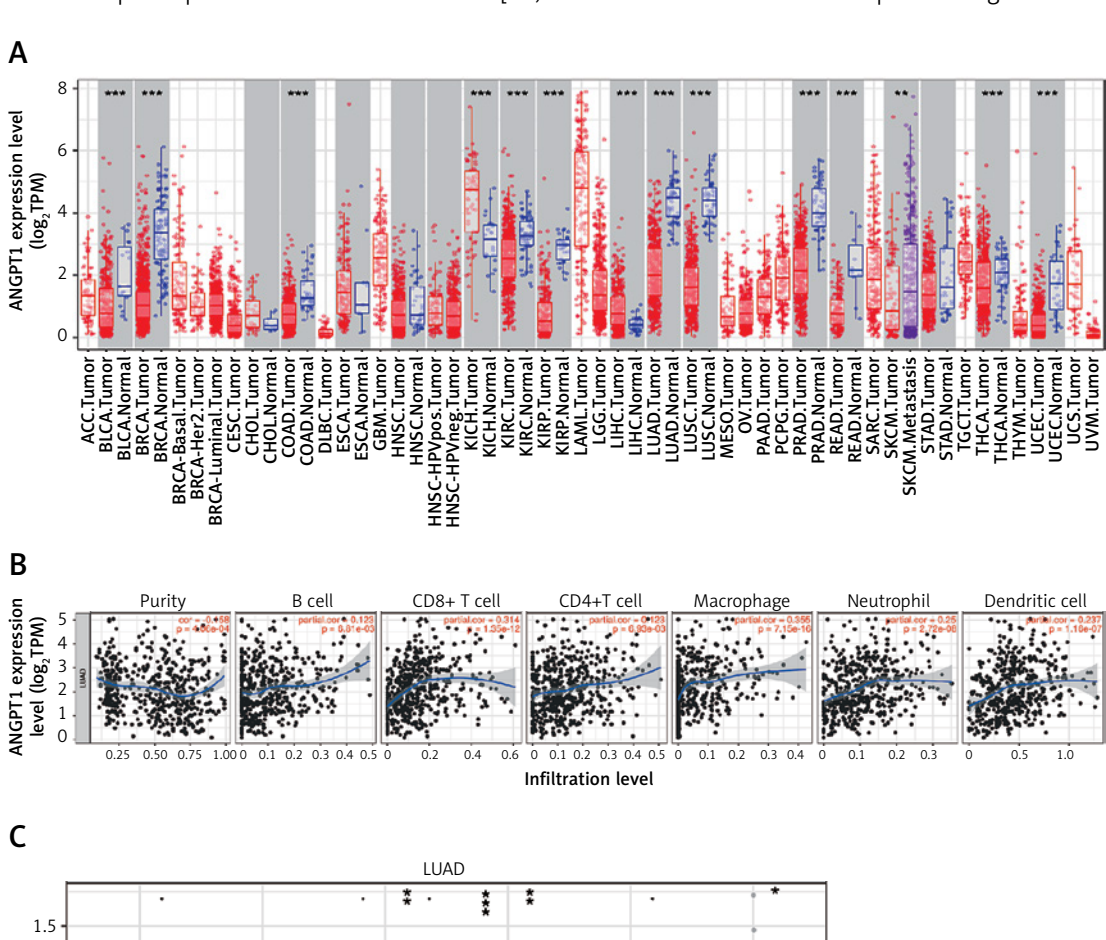


Figure 5. Cont. I – Associations between ANGPT1 expression and methylation and mutation levels in LUAD

signaling pathway [24, 25], MARK pathway [26], and cell adhesion. Three IncRNAs (AC008268.1, AFAP1-AS1, BLACAT1) were included in the TCGA database and m6A-related non-coding genes. However, only two IncRNAs (AFAP1-AS1, BLACAT1) were related to the prognosis of LUAD patients. Some studies have shown that AFAP1-AS1 and BLACAT1 participated in different cancers [27,

28]. Combining functional and prognostic analysis, we selected ANGPT1 as the targeted molecule. Through various databases, we found that ANGPT1 expression was lower in LUAD tissues than normal lung tissues (p < 0.01). The ceRNA network for ANGPT1 was constructed using various databases. In recent years, ceRNA networks have been shown to be important regulators in



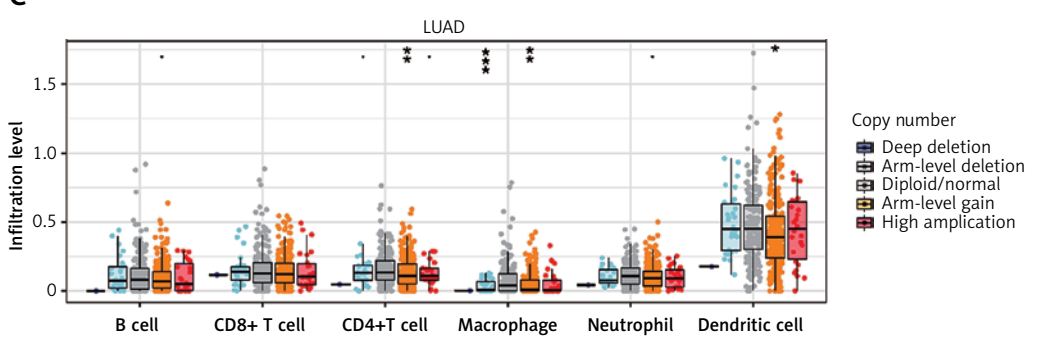


Figure 6. Correlation of ANGPT1 expression and immune cell infiltration. A – ANGPT1 expression in TIMER database. B, C – Associations between ANGPT1 expression and immune cells (p < 0.01)

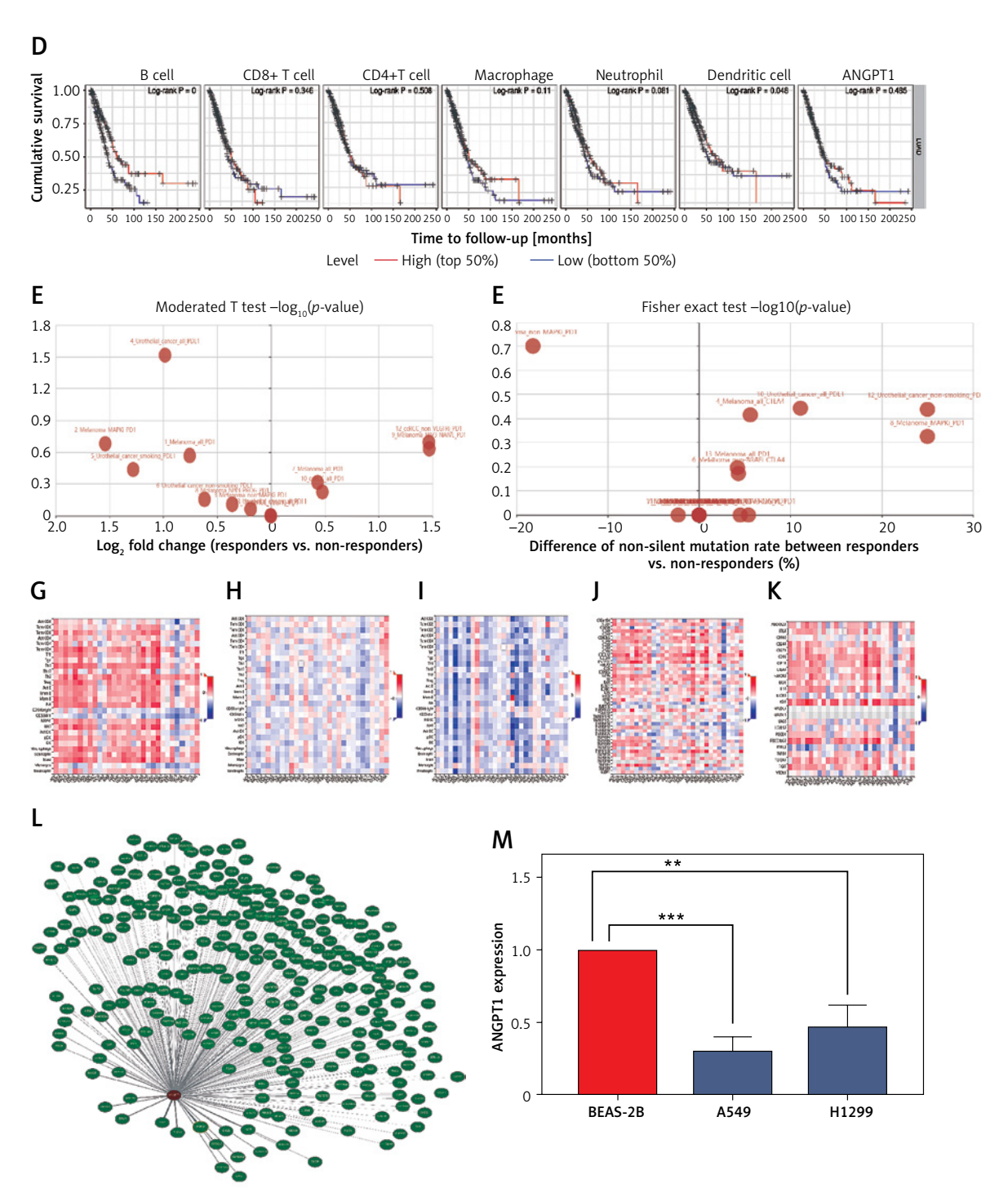


Figure 6. Cont. D – Associations between ANGPT1 expression and immune cells (p < 0.01). E, F – Difference in expression between PD-L1 responders and non-responders. G–K – Relationships between ANGPT1 expression and immune inhibitors and immune stimulators. L – Identification of immune-related co-expression gene network. M – ANGPT1 expression was lower in tumor tissues (A549 and H1299 cell lines) than normal lung tissues (BEAS-2B cell line), as demonstrated by PCR verification

cancers; for example, lncRNA HOTAIR functions as a ceRNA to regulate HER2 expression by sponging miR-331-3p in gastric cancer [29]. In our study, miRNA 448 [30] was found to act as a sponge to regulate ANGPT1 in LUAD. Contextualizing miR-448, it has been previously implicated in other cancer types. Its known roles often involve tar-

geting oncogenes or tumor suppressors related to apoptosis and proliferation. We are the first to identify and propose miR-448 as a direct regulator of ANGPT1 specifically in LUAD. More importantly, we place this miRNA-mRNA interaction within a broader regulatory context – the m6A-modified ceRNA network. We hypothesize that the m6A

Table II. Relations of ANGPT1 expression and multiple immune cell purity in LUAD

Cancer	Variable	Partial.cor	<i>P</i> -value
LUAD	Purity	-0.158489535	0.000406148
LUAD	B cell	0.122851718	0.006809772
LUAD	CD8+ T cell	0.313886112	1.35E-12
LUAD	CD4+ T cell	0.1225802	0.006934358
LUAD	Macrophage	0.355243102	7.15E-16
LUAD	Neutrophil	0.249550125	2.72E-08
LUAD	Dendritic cell	0.237070154	1.16E-07

modification on the lncRNAs identified in our network may influence their stability or their ability to sponge miR-448, thereby adding a critical layer of epitranscriptomic regulation to the control of ANGPT1 expression. This moves beyond a simple miRNA-target relationship and proposes a sophisticated multi-component regulatory circuit. Most significantly, our study is the first to connect this novel miR-448/ANGPT1 axis to the regulation of tumor immune infiltration. We propose that this axis represents a crucial link between RNA epigenetics (m6A), post-transcriptional regulation (ceRNA crosstalk), and immune remodeling. This provides a fundamentally new perspective on potential mechanisms of immune modulation in LUAD.

During cancer progression, tumor cells develop several mechanisms to prevent killing and to shape the immune system into a tumor-promoting environment [31]. Various immune cells (macrophages, neutrophils, dendritic cells, natural killer cells) influence the tumor microenvironment. Different immune microenvironments may have different reactivity to immunotherapy [32]. We studied the correlation between ANGPT1 expression and various immune cells: B cells (p = 4.06e-04), CD8+ T cells (p = 1.35e-12), CD4+ T cells (p = 6.93e-03), macrophages (p = 7.15e-16), neutrophils (p = 2.72e-3), and dendritic cells (p =1.16e-07). ANGPT1 was a prognostic immune-related biomarker and potential immunotherapy target. Beyond its well-established role in angiogenesis and vascular stability, our bioinformatic findings prompted us to investigate and discuss the potential immunomodulatory functions of ANGPT1 in the LUAD TME in greater depth. In our research, we propose a dual mechanistic model: 1) Indirect modulation via vascular normalization: We elaborate on the hypothesis that the loss of ANGPT1, a key agonist for the Tie2 receptor, likely contributes to aberrant, leaky, and immature tumor vasculature. This dysfunctional state creates a hypoxic and immunosuppressive TME. It acts as a physical barrier, hindering the infiltration of cytotoxic T cells and other anti-tumor immune effectors into the tumor core while promoting the recruitment of pro-tumorigenic immune cells such as M2 macrophages and regulatory T cells. Therefore, the downregulation of ANGPT1 we observed may not just be a passenger effect but an active driver of an immune-excluded phenotype, potentially explaining the resistance to immunotherapy observed in many LUAD patients; 2) Direct immunomodulatory signaling: Furthermore, emerging evidence suggests that the ANGPT1/Tie2 axis is not limited to endothelial cells. Tie2 is expressed on a subset of pro-angiogenic and immunosuppressive macrophages (often referred to as Tie2-expressing macrophages). Signaling through this receptor can promote a pro-tumorigenic M2like polarization. The downregulation of ANGPT1 in tumor cells could potentially disrupt this signaling axis, but the net effect on the immune landscape is complex and context-dependent. We discuss this nuance, stating that our observed correlations suggest a significant, albeit complex, role for ANGPT1 in shaping the immune contexture of LUAD. Construction of the immune-related ceRNA network provided a novel insight for revealing potential immune therapeutic targets in RNA epigenetics [33].

ANGPT1 has been implicated in various diseases, such as hereditary angioedema [34], breast cancer [35], and colorectal cancer [36]. However, the underlying mechanism of ANGPT1 involvement remained unclear. The advantage of our study was that, for the first time, we constructed an m6A-related ceRNA network focused on ANGPT1. We combined immune, methylation, and m6A databases, and deeply analyzed ANGPT1-related gene epigenetic characteristics. The relationships of ANGPT1 expression and immune infiltrating cells were shown in detail in our research (p < 0.01). A signature of m6A-related ceRNA network provided a new vision for immunotherapy of LUAD. Bioinformatics and basic experimental verification improve the reliability of our study.

This study identified ANGPT1-related ceRNA networks and their immune correlations in LUAD. However, several limitations should be acknowledged: The predicted m6A-mediated regulatory relationships (miR-448/ANGPT1 axis) requires exper-

imental validation using RIP-seq or dual-luciferase assays. The findings rely on TCGA/GEO bioinformatics analyses. Inclusion of multicenter clinical cohorts could strengthen prognostic generalizability.

In summary, we identified differentially expressed m6A-related mRNAs and long non-coding RNAs and constructed a ceRNA network. Focusing on ANGPT1, we found an association between its expression and immune cells (p < 0.01). We identified ANGPT1-related co-expression genes (2) using Coexpedia in LUAD, which provided novel insights regarding new therapeutic targets.

In conclusion, by integrating TCGA, GEO, CIBER-SORTx, and Coexpedia databases, we identified an ANGPT1-associated ceRNA network and co-expression genes. These molecules show significant correlations with immune infiltration levels and may represent RNA epigenetics-based regulatory candidates. Further experimental validation is needed to confirm their mechanistic roles.

Acknowledgments

The authors are grateful to the investigators of the original studies for sharing the public database statistics. Zhuohui Tan and Chunhong Fan contributed equally. Zhuohui Tan and Chunhong Fan share first authorship.

Funding

No external funding.

Ethical approval

Not applicable.

Conflict of interest

The authors declare no conflict of interest.

References

- 1. Mukhopadhyay D, Cocco P, Orrù S, Cherchi R, De Matteis S. The role of MicroRNAs as early biomarkers of asbestos-related lung cancer: a systematic review and meta-analysis. Pulmonology 2025; 31: 2416792.
- Tang JN, Kong DG, Cui QX, et al. Prognostic genes of breast cancer identified by Gene Co-expression Network Analysis. Front Oncol 2018; 8: 374.
- Xu ZQ, Li JW, Fang SY, et al. Cinobufagin disrupts the stability of lipid rafts by inhibiting the expression of caveolin-1 to promote non-small cell lung cancer cell apoptosis. Arch Med Sci 2024; 20: 887-908.
- Dong HX, Wang R, Jin XY, Zeng J, Pan J. LncRNA DGCR5 promotes lung adenocarcinoma (LUAD) progression via inhibiting hsa-mir-22-3p. J Cell Physiol 2018; 233: 4126-36.
- Fu LH, Wang HY, Wei DS, et al. The value of gene as a diagnostic biomarker and independent prognostic factor in LUAD and LUSC. PLoS One 2020; 15: e0233283.
- Ma LF, Zhang X, Yu KK, et al. Targeting SLC3A2 subunit of system Xis essential for mA reader YTHDC2 to be an en-

- dogenous ferroptosis inducer in lung adenocarcinoma. Free Radical Bio Med 2021; 168: 25-43.
- Galazka JK, Czeczelewski M, Kucharczyk T, Szklener K, Mandziuk S. Obesity and lung cancer - is programmed death ligand-1 (PD-1L) expression a connection? Arch Med Sci 2024; 20: 313-6.
- Yu L, Qiao R, Xu JL, Han BH, Zhong RB. FAM207BP, a pseudogene-derived lncRNA, facilitates proliferation, migration and invasion of lung adenocarcinoma cells and acts as an immune-related prognostic factor. Life Sci 2021; 268: 119022.
- Zhang YY, Liu X, Liu LW, Li JH, Hu QY, Sun RR. Expression and prognostic significance of m6A-related genes in lung adenocarcinoma. Med Sci Monitor 2020; 26: e919644.
- Li Y, Gu J, Xu FK, et al. Molecular characterization, biological function, tumor microenvironment association and clinical significance of mA regulators in lung adenocarcinoma. Brief Bioinform 2021; 22: bbaa225.
- 11. Ma LF, Chen TX, Zhang X, et al. The mA reader YTHDC2 inhibits lung adenocarcinoma tumorigenesis by suppressing SLC7A11-dependent antioxidant function. Redox Biol 2021; 38: 101801.
- Han J, Wang JZ, Yang X, et al. METTL3 promote tumor proliferation of bladder cancer by accelerating primiR221/222 maturation in m6A-dependent manner. Mol Cancer 2019; 18: 110.
- Guo XY, Li K, Jiang WL, et al. RNA demethylase ALKBH5 prevents pancreatic cancer progression by posttranscriptional activation of PER1 in an m6A-YTHDF2-dependent manner. Mol Cancer 2020; 19: 91.
- Zhang C, Zhang MQ, Ge S, et al. Reduced m6A modification predicts malignant phenotypes and augmented Wnt/PI3K-Akt signaling in gastric cancer. Cancer Med 2019; 8: 4766-81.
- 15. Qi XL, Zhang DH, Wu N, Xiao JH, Wang X, Ma W. ceRNA in cancer: possible functions and clinical implications. J Med Genet 2015; 52: 710-8.
- Luan XT, Wang YK. LncRNA XLOC_006390 facilitates cervical cancer tumorigenesis and metastasis as a ceRNA against miR-331-3p and miR-338-3p. J Gynecol Oncol 2018; 29: e95.
- Zhang K, Zhang L, Mi Y, et al. A ceRNA network and a potential regulatory axis in gastric cancer with different degrees of immune cell infiltration. Cancer Sci 2020; 111: 4041-50.
- 18. Hinshaw DC, Shevde LA. The tumor microenvironment innately modulates cancer progression. Cancer Res 2019; 79: 4557-66.
- 19. Bader JE, Voss K, Rathmell JC. Targeting metabolism to improve the tumor microenvironment for cancer immunotherapy. Mol Cell 2020; 78: 1019-33.
- 20. Rusk N. Expanded CIBERSORTx. Nat Methods 2019; 16: 577.
- 21. Chandrashekar DS, Bashel B, Balasubramanya SAH, et al. UALCAN: a portal for facilitating tumor subgroup gene expression and survival analyses. Neoplasia 2017; 19: 649-58.
- 22. Vacek J, Liesveld J. Teaching concepts to nursing students using model case studies, the venn diagram, and questioning strategies. Nurs Educ Perspect 2020; 41: 373-5.
- 23. Li B, Severson E, Pignon JC, et al. Comprehensive analyses of tumor immunity: implications for cancer immunotherapy. Genome Biol 2016; 17: 174.
- 24. Xie YB, Shi XF, Sheng K, et al. PI3K/Akt signaling transduction pathway, erythropoiesis and glycolysis in hypoxia. Mol Med Rep 2019; 19: 783-91.

- 25. Tang JM, Cao Y, Zhang H, Wang R. Oxymatrine inhibits the development of radioresistance in NSCLC cells by reversing EMT through the DcR3/AKT/GSK-3β pathway. Arch Med Sci 2024; 20: 1631-54.
- Kist M, Vucic D. Cell death pathways: intricate connections and disease implications. Embo J 2021; 40: 106700.
- 27. Han ML, Gu YT, Lu PW, et al. Exosome-mediated lncRNA AFAP1-AS1 promotes trastuzumab resistance through binding with AUF1 and activating ERBB2 translation (Retraction of Vol 19, 10.1186/S12943-020-1145-5, 2020). Mol Cancer 2022; 19: 26.
- 28. Lu HY, Liu HR, Yang XQ, et al. LncRNA BLACAT1 may serve as a prognostic predictor in cancer: evidence from a meta-analysis. Biomed Res Int 2019; 2019: 1275491.
- Liu XH, Sun M, Nie FQ, et al. Lnc RNA HOTAIR functions as a competing endogenous RNA to regulate HER2 expression by sponging miR-331-3p in gastric cancer. Mol Cancer 2014; 13: 92.
- 30. Liao ZB, Tan XL, Dong KS, et al. miRNA-448 inhibits cell growth by targeting BCL-2 in hepatocellular carcinoma. Digest Liver Dis 2019; 51: 703-11.
- Bärenwaldt A, Läubli H. The sialoglycan-Siglec glyco-immune checkpoint a target for improving innate and adaptive anti-cancer immunity. Expert Opin Ther Tar 2019; 23: 839-53.
- 32. Wu DJ. Innate and adaptive immune cell metabolism in tumor microenvironment. Adv Exp Med Biol 2017; 1011: 211-23.
- Nebbioso A, Tambaro FP, Dell'Aversana C, Altucci L Cancer epigenetics: moving forward. Plos Genet 2018; 14: e1007362.
- 34. Bafunno V, Firinu D, D'Apolito M, et al. Mutation of the angiopoietin-1 gene associates with a new type of hereditary angioedema. J Allergy Clin Immun 2018; 141: 1009-17.
- 35. Flores-Pérez A, Marchat LA, Rodríguez-Cuevas S, et al. Dual targeting of ANGPT1 and TGFBR2 genes by miR-204 controls angiogenesis in breast cancer. Sci Rep 2016; 6: 34504.
- 36. Dai JY, Wan SG, Zhou F, et al. Genetic polymorphism in a VEGF-independent angiogenesis gene ANGPT1 and overall survival of colorectal cancer patients after surgical resection. PLoS One 2012; 7: e34758.